Proceedings of the 7th International Symposium on Steel Science (ISSS 2024)
Nov. 11-14, 2024, Kyoto, Japan: The Iron and Steel Institute of Japan

In situ neutron diffraction study to elucidate hydrogen effect on the deformation mechanism in Type 310S austenitic stainless steel

Tatsuya Ito[1*], Yuhei Ogawa[2], Wu Gong[2], Wenqi Mao[2], Takuro Kawasaki[2], Kazuho Okada[2], Akinobu Shibata[2], Stefanus Harjo[2]

[1] Japan Atomic Energy Agency, J-PARC Center, 2-4 Shirakata, Tokai-mura, Naka-gun, Ibaraki, Japan
[2] National Institute for Materials Science, Research Center for Structural Materials, 1-2-1 Sengen, Tsukuba, Ibaraki, Japan

Abstract:

Hydrogen embrittlement has long been an obstacle to the development of safe infrastructure. However, in contrast to hydrogen's embrittling effect, recent research has revealed that the addition of hydrogen improves both the strength and uniform elongation of AISI Type 310S austenitic stainless steel. A detailed understanding of how hydrogen affects the deformation mechanism of this steel could pave the way for the development of more advanced materials with superior properties. In the present study, *in situ* neutron diffraction experiments were conducted on Type 310S steel with and without hydrogen-charged to investigate the effect of hydrogen on the deformation mechanism. In addition to the effect of solid-solution strengthening by hydrogen, the q-value, a parameter representing the proportion of edge and screw dislocations in the accumulated dislocations, was quantitatively evaluated using CMWP analysis on neutron diffraction patterns. The comparison of q-values between the hydrogen-charged and non-charged samples reveals that hydrogen has minimal effect on dislocation character in Type 310S steel.

1. INTRODUCTION

Hydrogen is being considered as alternative carrier to fossil fuels in achieving the goal of “carbon neutrality”. The construction of a safe hydrogen infrastructure is crucial for realizing a hydrogen-based society [1]. However, hydrogen is closely associated with steel embrittlement, referred to as "hydrogen embrittlement," which remains a key challenge in developing safe infrastructure [2].

In contrast to the typical understanding of the hydrogen embrittlement, Ogawa *et al.* recently reported that the addition of hydrogen to AISI Type 310S steel enhances both strength and uniform elongation [3]. The increase in strength was attributed to solid-solution strengthening by hydrogen [3,4], while the improvement in uniform elongation was explained by an increased work-hardening rate due to hydrogen-assisted deformation twinning [3,5]. This phenomenon has attracted attention as a potential method to overcome hydrogen embrittlement. A detailed understanding of hydrogen’s impact on the deformation mechanism in Type 310S steel is crucial for developing steel materials with improved properties.

To elucidate hydrogen effect on the deformation mechanism, it is crucial to investigate the influence of hydrogen on crystal defects such as dislocations and stacking faults. Recently, our group conducted in situ neutron diffraction experiments on hydrogen-charged Type 310S steel to investigate the impact of hydrogen on these crystal defects. We analyzed the lattice constant, lattice strain, stacking fault probability/energy, twin evolution stress, and dislocation density from the obtained neutron diffraction patterns, and the results will be reported elsewhere [6]. However, the effect of hydrogen on dislocation characteristics, such as the ratio of edge to screw dislocations in Type 310S steel, remains unclear. In the case of ferritic steel, neutron diffraction and transmission electron microscopy observations have demonstrated that hydrogen has a substantial impact on the characteristics of accumulated dislocations [7]. In contrast, in austenitic Type 316L steel, it has been reported that hydrogen does not influence the proportion of screw or edge dislocations [8]. These differences are believed to arise from the crystal structure, but the details remain unclear, and further data collection across various alloy systems is necessary. In this study, we evaluated the effect of hydrogen on the dislocation characteristics of Type 310S austenitic steel using *in situ* neutron diffraction.

* Corresponding author. E-mail: tatsuya.ito@j-parc.jp, telephone: +81 29 284 3199.

https://doi.org/10.2355/isijisss.2024.0_237

2. EXPERIMENTAL PROCEDURES

2.1. Samples

Round bar tensile samples of Type 310S austenitic steel were fabricated from a 20 mm-diameter rod that was solution heat-treated at 1080°C for 2 minutes, followed by water quenching. The chemical composition of the sample is shown in Table 1. The parallel section of the sample measured 6 mm in diameter and 30 mm in length. The sample was exposed to hydrogen gas at 270°C and 100 MPa for 200 hours, conditions suitable for achieving a uniform hydrogen concentration in the parallel section of the sample [5]. The hydrogen concentration was analyzed using Thermal Desorption Spectroscopy (TDS) with a gas chromatography system featuring a thermal conductivity detector (JTF-20A, J-SCIENCE LAB Co., Ltd., Japan). The hydrogen concentration in the hydrogen-charged (H-charged) sample was measured at 139±1 mass ppm, while it was 4.5±0.5 mass ppm in the non-charged sample.

Table 1. Chemical compositions of the sample (mass %)

Fe	Ni	Cr	Mn	Si	C	P	S
Bal.	19.2	24.2	1.10	0.37	0.02	0.02	0.001

2.2. In situ neutron diffraction

Figure 1(a) shows the schematic illustration of the Engineering Materials Diffractometer, TAKUMI, at the Materials and Life Science Experimental Facility (MLF) of the Japan Proton Accelerator Research Complex (J-PARC). This equipment enables us to obtain neutron diffraction data during continuous deformation. The North (-90°) detector bank measures the lattice spacing parallel to the loading direction (LD), while the South (+90°) detector bank measures it in the transverse direction (TD). In this study, we analyzed data corrected from the North detector bank. The incident beam size was set to a width of 5 mm and a height of 8mm using the slit, and a pair of radial collimators viewing a 5 mm width was used.

In situ neutron diffraction measurements during tensile testing were conducted for both H-charged and non-charged samples. The crosshead speed was set to 0.05 mm/min, corresponding to an initial strain rate of 3×10^{-5} sec^{-1}. The strain of the sample was measured using the digital image correlation (DIC) technique [9]. The true stress-strain curves during uniform elongation of the samples are shown in Figure 1(b) [6]. Both strength and uniform elongation were enhanced by hydrogen addition, consistent with the previous study [3].

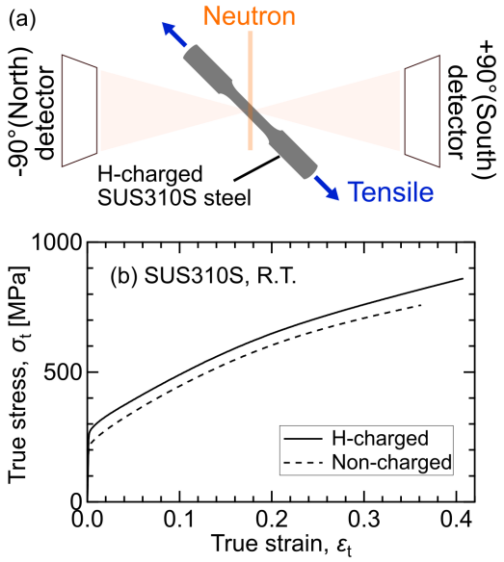

Figure 1. (a) The schematic illustration of the setup for *in situ* neutron diffraction measurements using the Engineering Materials Diffractometer, TAKUMI. (b) True stress-strain curves for the H-charged (solid line) and non-charged (dotted line) samples during *in situ* neutron diffraction experiments [6].

2.3. Analysis

Time-sliced *in situ* neutron diffraction patterns during plastic deformation were obtained with slice intervals ranging from 90 to 300 seconds, depending on the stress variation within the selected ranges. The time-sliced data were then used to analyze dislocation characteristics through the Convolutional Multiple Whole Profile (CMWP) method, which applies a convolutional profile fitting method based on Wilkens theory [10,11]. The "q-values", indicating the proportion of edge and screw dislocations [10], were obtained from the fitting results. For austenitic stainless steel, the q-value is 1.55 for pure edge dislocations and 2.53 for pure screw dislocations [12]. In the CMWP analysis, the evaluation is based on changes in diffraction profile shape, although it is known that planar defects, such as stacking faults, can also affect the peak shape [13]. In this study, the stacking fault probability (P_{SF}) was calculated using the procedure outlined below, and the CMWP analysis was performed considering the changes in peak shape.

The presence of stacking faults causes shifts in peak positions, and the magnitude of peak shift depends on both the P_{SF} and the peak index [14]. The P_{SF} can be evaluated using the following equation, which incorporates the apparent lattice strain (ε^{hkl}) [15,16]:

$$P_{SF} = \frac{32\pi}{3\sqrt{3}}(\varepsilon^{222} - \varepsilon^{111}). \quad (1)$$

The ε^{hkl} can be calculated as follows:

$$\varepsilon^{hkl} = \frac{d^{hkl} - d_0^{hkl}}{d_0^{hkl}}, \quad (2)$$

where d^{hkl} and d_0^{hkl} represent the apparent lattice (*d*-) spacings during and before deformation, respectively, as analyzed using Z-Rietveld software [17]. This evaluation method eliminates the peak shift caused by stress, as the two reflections from the same crystal plane (*i.e.*, 111 and 222) experience the same magnitude of stress in this experimental setup (Figure. 1(a)).

3. RESULTS AND DISCUSSION

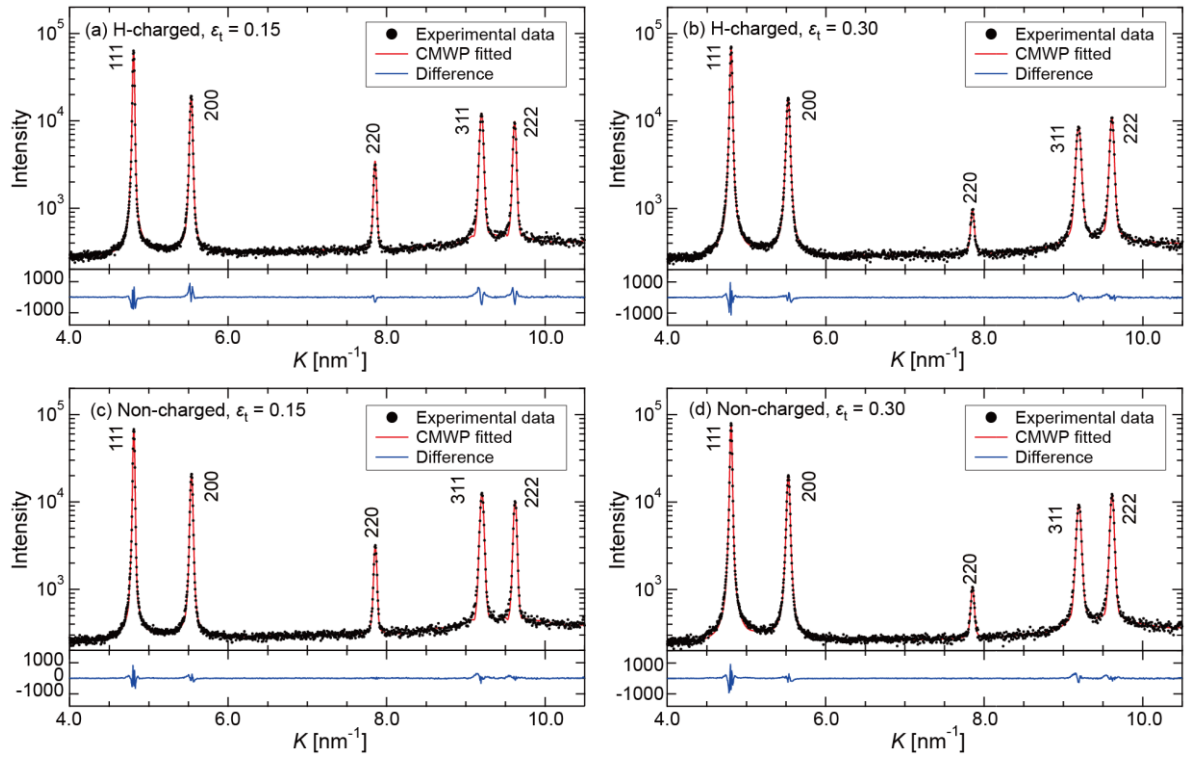

Figure 2. Typical *in situ* neutron diffraction patterns for the (a, b) H-charged and (c, d) non-charged samples, with applied true strains (ε_t) of (a, c) 0.15 and (b, d) 0.30, respectively. The experimental data are represented by black points, while the CMWP fitting results and the differences are shown by red and blue lines, respectively.

Figure 2 illustrates *in situ* neutron diffraction patterns obtained during tensile testing. Figures 2(a) and 2(b) show the results for the H-charged sample at true strains (ε_t) of 0.15 and 0.30, respectively, while Figures 2(c) and 2(d) show the results for the non-charged sample at the same true strain levels. The experimental data are shown as black points, with the fitting results shown as red lines. The differences between them are displayed at the bottom as blue lines. The experimental results are plotted on a logarithmic scale, while the differences are plotted on a linear scale. As deformation progresses, the peak width gradually increases, suggesting the accumulation of dislocations. The lattice constants of the H-charged and non-charged samples, measured before deformation, were used to calculate the volume expansion per solute hydrogen atom, which was obtained to be 2.27 ± 0.02 Å^3 per H-atom [6]. Lattice strains were evaluated based on the shifts in diffraction peaks. In the H-charged sample, the lattice strains deviated from the linear elastic region at higher stress levels compared to the non-charged

sample. This indicates an increase in the elastic limit or yield strength due to solid-solution hardening [6].

Figure 3 shows the evaluated q-values as a function of true strain. The solid circles show the result of the H-charged sample, while open circles correspond to the non-charged sample. As deformation progresses, the q-value gradually decreased, suggesting an increasing edge dislocation component, which is consistent with findings in Type 316L steel [8]. The lack of a noticeable difference between the plots of the H-charged and non-charged materials samples indicates that 139 mass ppm of hydrogen has minimal impact on the proportion of edge and screw dislocations. This negligible influence is consistent with findings reported in Type 316L steel analyzed by X-ray diffraction [8]. Furthermore, we evaluated the dislocation density and work-hardening behavior due to dislocation storage and found that the effect of hydrogen was negligible [6]. These results imply that the changes in mechanical properties due to hydrogen are not caused by its effect on dislocations, but rather by other factors, such as solid-solution strengthening and deformation twinning, as discussed in our other papers [6]. The minimal change in dislocation character observed in austenitic steels, such as Type 310S (this study) and Type 316L [8], indicate that the hydrogen effect is less pronounced in austenitic stainless steel, in contrast to its significant effect on ferritic steel [7]. Clarifying the reasons for these differences will help improve our understanding of hydrogen–dislocation interactions.

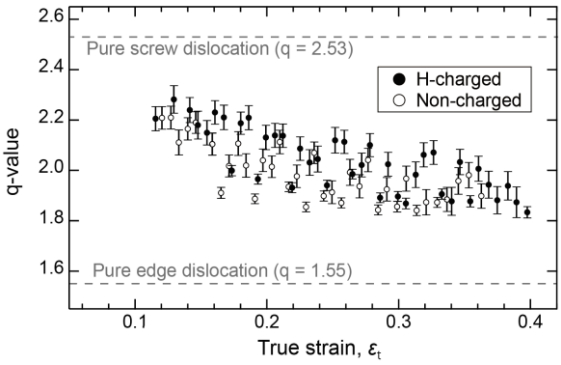

Figure 3. The q-value of the H-charged (solid circles) and non-charged (open circles) samples.

4. CONCLUSIONS

In this study, the influence of hydrogen on the proportion of dislocation characteristics was examined through in situ neutron diffraction using TAKUMI. CMWP analysis of the neutron diffraction patterns revealed that 139 mass ppm of hydrogen has a minimal effect on the stored dislocation characteristics in Type 310S steel.

Acknowledgements: This research was supported by JSPS Grant-in-Aid for Research Activity Start-up (JP23K19189), JSPS Grant-in-Aid for Early-Career Scientists (JP21K14045), Iketani Science and Technology Foundation (0361224-A), and MEXT Program: Data Creation and Utilization Type Material Research and Development (JPMXP1122684766). The neutron diffraction experiment at the MLF of the J-PARC was performed under proposal number 2023I0019.

REFERENCES

[1] H. Li, X. Cao, Y. Liu, Y. Shao, Z. Nan, L. Teng, W. Peng, J. Bian: Energy Rep., 8 (2022), 6258–6269.
[2] X. Li, X. Ma, J. Zhang, E. Akiyama, Y. Wang, X. Song: Acta. Metall. Sin. (Engl. Lett.), 33 (2020), 759–773.
[3] Y. Ogawa, H. Hosoi, K. Tsuzaki, T. Redarce, O. Takakuwa, H. Matsunaga: Acta Mater., 199 (2020), 181–192.
[4] D.P. Abraham, C.J. Altstetter: Metall. Mater. Trans. A, 26 (1995), 2849–2858.
[5] Y. Ogawa, H. Nishida, O. Takakuwa, K. Tsuzaki: Mater. Today Commun., 34 (2023), 105433.
[6] T. Ito, Y. Ogawa, W. Gong, W. Mao, T. Kawasaki, K. Okada, A. Shibata, S. Harjo: Submitted.
[7] K. Okada, A. Shibata, W. Gong, N. Tsuji: Acta Mater., 225 (20022) 117549.
[8] K. Kamei, Y. Koumura, A. Macadre, K. Goda: ISIJ Int., 61 (2021), 1736–1738.
[9] W. Mao, W. Gong, T. Kawasaki, S. Harjo: Mater. Sci. Eng. A, 837 (2022), 142758.
[10] T. Ungár, J. Gubicza, G. Ribárik, A. Borbély: J. Appl. Crystallogr., 34 (2001), 298–310.
[11] G. Ribárik, J. Gubicza, T. Ungár: Mater. Sci. Eng. A, 387–389 (2004), 343–347.
[12] M. Moshtaghi, S. Sato: ISIJ Int., 59 (2019), 1591–1598.
[13] L. Balogh, G. Ribárik, T. Ungár: J. Appl. Phys., 100 (2006), 023512.
[14] B.E. Warren: X-ray diffraction, Courier Corporation (1990).
[15] W. Woo, J.S. Jeong, D.-K Kim, C.M. Lee, S.-H. Choi, J.-Y. Suh, S.Y. Lee, S. Harjo, T. Kawasaki: Sci. Rep., 10 (2020) 1350.
[16] W. Mao, S. Gao, W. Gong, T. Kawasaki, T. Ito, S. Harjo, N. Tsuji: Acta Mater., 278 (2024) 120233.
[17] R. Oishi-Tomiyasu, M. Yonemura, T. Morishima, A. Hoshikawa, S. Torii, T. Ishigaki, T. Kamiyama: J. Appl. Crystallogr., 45 (2012), 299–308.